Electronic Supplementary Material (ESI) for Lab on a Chip.

SUPPORTING INFORMATION

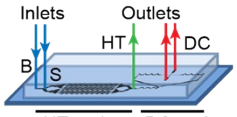

		Prime	Pressurize	Infuse	Wash	Stabilize	Release	Flush
		60s	30s	150s	15s	5s	1s	60s
In	Buffer solution (mL/min)	1	8	1	8	8	8	1
In	Sample solution (mL/min)	0	0	7	0	–0.5	0	0
Out	HT outlet (open/close)	✖	✓	✓	✓	✓	✖	✖
Out	DC outlet (open/close)	✓	✖	✖	✖	✓	✓	✓

Fig. S1. Device process flow. Samples are processed in a series of logical steps and require specific flow rates for the buffer (B) and sample (S), as well as specific valving configurations for the HT and DC outlets, as shown in the table. The process involves: i) priming the device to fill channels with fluid, ii) pressurizing the chambers at high flow rate to prevent contaminating back-flows, iii) infusing the patient sample to capture CTCs in vortices, iv) washing the reservoirs to remove unstably trapped smaller cells, v) stabilizing the sample syringe to reduce residual blood leakage, vi) releasing the cells from vortices and into the DC region of the device, and vii) flushing the system to ensure all cells are released into the downstream collection vessel. Solution flow rates and outlet valving must be controlled for each step.

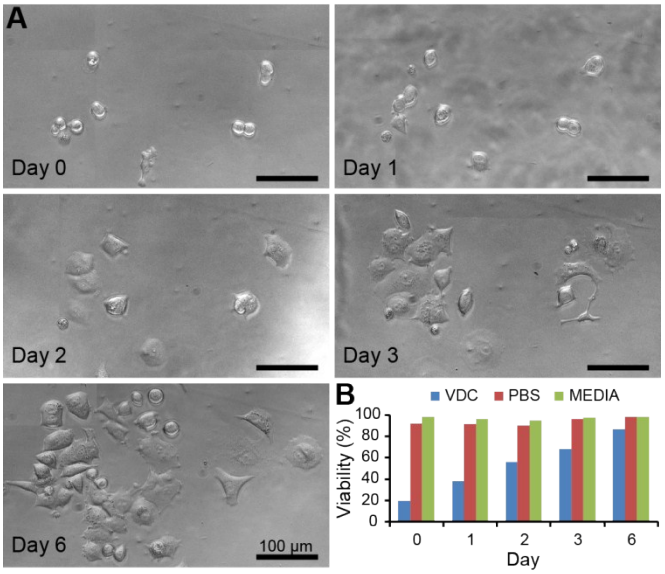

Fig. S2. Cell growth. (A) MCF7 cells collected from the VDC device adhered and proliferated in culture over the course of 6 days, at which point the experiment was stopped. (B) Apparent cell viability was low on Day 0 (blue) relative to unprocessed control cells resting in PBS (red) and media (green), but increased steadily. Viability increased before cell proliferation occurred (Day 3, 56%), indicating that cells may have become permeabilized and absorbed the dead stain before recovering. The additional increase in viability thereafter (up to 87%) may be due to the increased number of proliferated live cells.

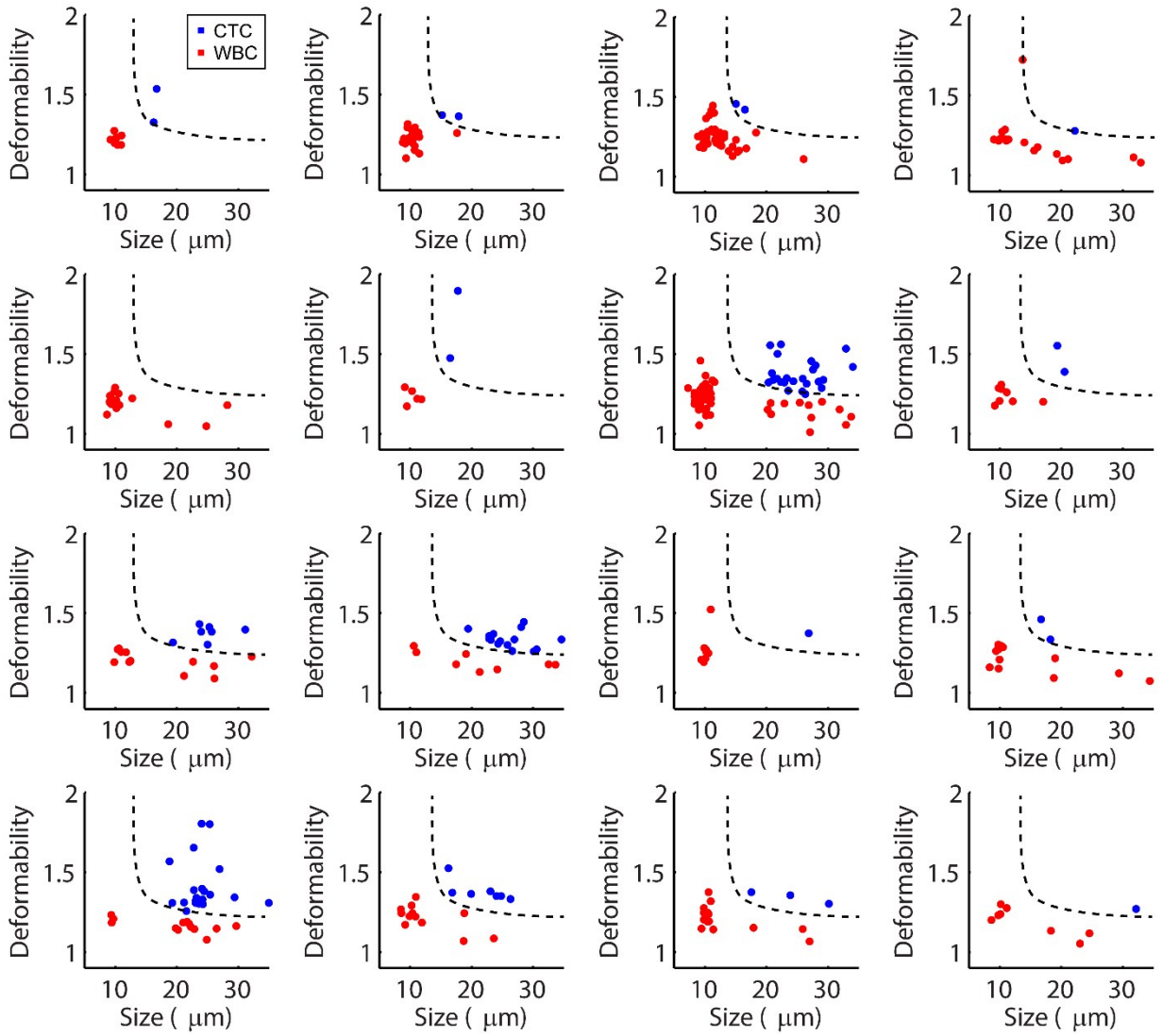

Fig. S3. Biophysical profiles of individual cancer patients. Each graph represents cells collected from one cancer patient blood donor in the study, which includes 16 samples. Each cell is plotted along a deformability versus size axis that includes a multiparameter threshold that distinguishes CTCs (blue) from non-CTCs (red), as illustrated in Figs. 3C, S5.

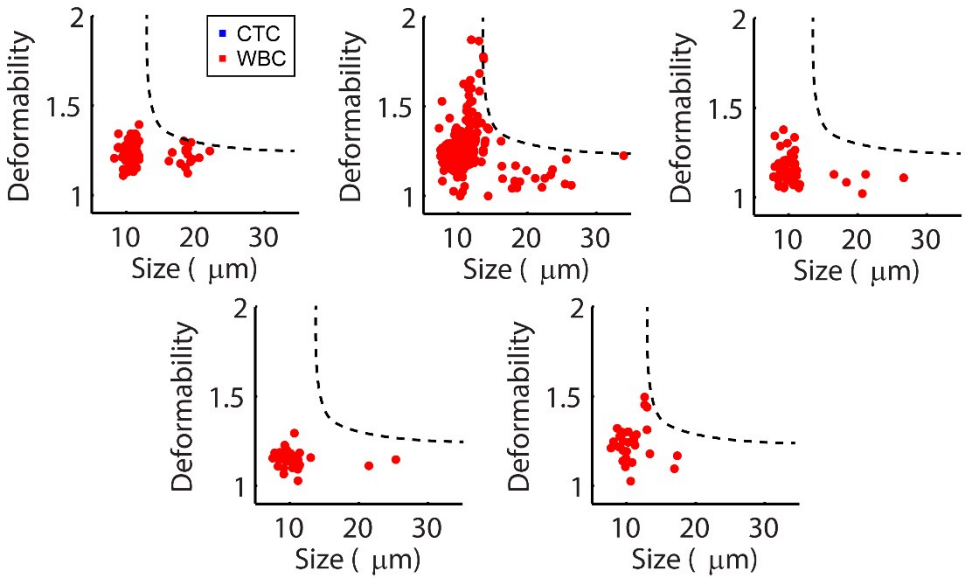

Fig. S4. Biophysical profiles of individual healthy patients. Similar to Fig. S3, each graph represents cells collected from each age-matched healthy blood donor in the study, which includes 5 samples. Each cell is plotted along a deformability versus size axis that includes a multiparameter threshold that distinguishes CTCs (blue) from non-CTCs (red), as illustrated in Figs. 3C, S5.

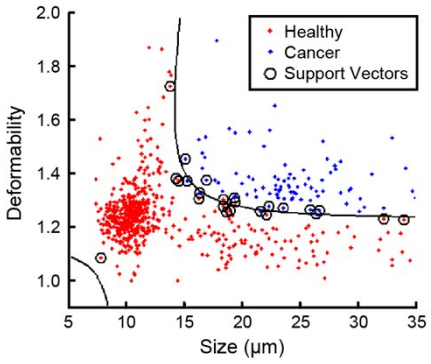

Fig. S5. SVM on VDC data. The graph shown displays the support vectors (circles) used to compute the threshold that distinguishes CTCs (blue) from healthy cells (red), using the MATLAB svmtrain function. The data points inputted were derived from healthy and cancer patient donor samples used in the study.

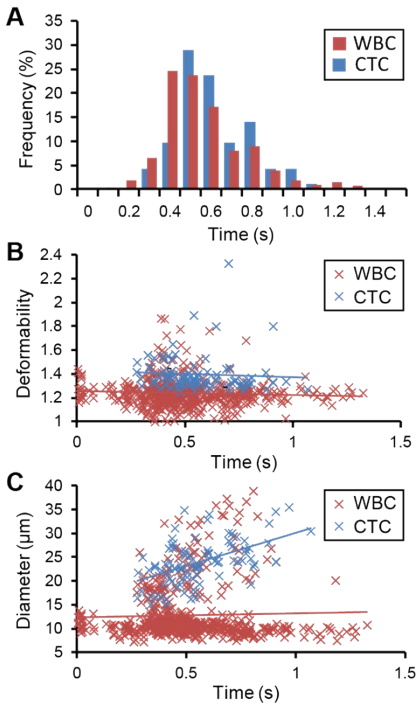

Fig. S6. Metrics of CTC occurrences in VDC video. (A) Similar to the measurements from cell line tests (Fig. 2B), CTCs and WBCs in VDC videos all appeared in a <1s time period. (B) There were no correlations of cell deformability with the time of appearance in the video for all cells in patient samples (R^2=0.0038 CTC, R^2=0.0047 WBC), suggesting that the slightly increasing flow speed during the course of cell release (Fig. 2E) was negligible to mechanophenotyping measurements. (C) The measured diameter of CTCs roughly correlated with time of appearance (R^2=0.26), which matched observations that larger cells were trapped closer toward the initial vortex reservoirs and further away from the DC junction, causing them to appear later in videos.

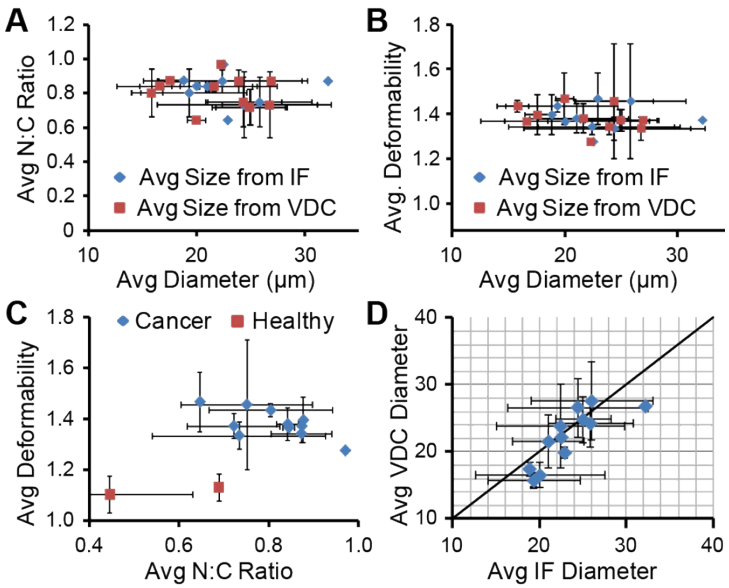

Fig. S7. Comparisons of VDC and IF metrics. The average size of CTCs measured from the well (blue) and from video (red) within each patient sample showed no correlation with (A) the average N:C ratio of cells, and (B) the average deformability of cells. (C) No clear trend was shown between the average deformability and average N:C ratio of each patient sample. (D) The average size of cells measured in VDC and IF were roughly correlated ($R^2 = 0.67$).

SUPPORTING TABLES

Table S1. Summary of patient blood samples processed in the study. 5 healthy and 16 stage IV NSCLC samples were processed through VDC and collected in a well plate for IF analysis. Over the course of the study, small adjustments to the VDC processing protocol were made to significantly decrease WBC contamination during the release, enabling WBC counts in the well plate. IF data could not be produced from 2 samples (marked N/A).

No.	Type	Vol. (mL)	VDC	IF		CTCs/mL	
			CTC count	CTC count	WBC count	VDC	IF
1	NSCLC	4	2	1	lots	0.5	0.25
2	NSCLC	6	2	1	lots	0.33	0.17
3	NSCLC	4	2	2	lots	0.5	0.5
4	NSCLC	8	1	1	lots	0.13	0.13
5	NSCLC	6	0	0	lots	0	0
6	NSCLC	8	2	N/A	N/A	0.25	N/A
7	NSCLC	12	24	N/A	N/A	2	N/A
8	NSCLC	14	2	1	lots	0.14	0.07
9	NSCLC	4	7	6	lots	1.75	1.5
10	NSCLC	6	16	15	274	2.67	2.5
11	NSCLC	8	1	1	424	0.13	0.13
12	NSCLC	8	2	1	127	0.25	0.13
13	NSCLC	14	21	20	240	1.5	1.43
14	NSCLC	12	7	4	160	0.58	0.33
15	NSCLC	16	3	3	186	0.19	0.19
16	NSCLC	16	1	0	229	0.06	0
17	Healthy	8	0	0	294	0	0
18	Healthy	8	0	0	236	0	0
19	Healthy	8	0	1	679	0	0.13
20	Healthy	8	0	0	79	0	0
21	Healthy	8	0	0	45	0	0

SUPPORTING VIDEOS

Video S1. VDC process flow. Video showing the steps of sample infusion, solution exchange, and release from a reservoir in the Vortex HT region of the device. During release, cells transfer to the DC region, where they are deformed. Video frame rate has been scaled at each step for appropriate visualization of events.

Video S2. Visualization of cell deformability. Video of representative CTCs from clinical samples, WBCs, and large non-CTCs from healthy samples.